

HEAT AND MASS TRANSFER ANALYSIS ON MAGNETO HYDERO POROUS CHANNEL WITH THERMAL RADIATION DYNAMIC PERISTALTIC FLUID FLOW THROUGH

Mantha Srikanth¹, Ashfar Ahmed², Dr. P. Sarada Devi³, Dr. P. J. Ravindranath⁴

Assistant Professor, Malla Reddy Engineering College (Autonomous), Hyderabad, Telangana, India.

manthasrikant9@gmail.com

Assistant Professor, Malla Reddy Engineering College (Autonomous), Hyderabad, Telangana, India.

ahmedashfaq02@gmail.com

Assistant Professor, Malla Reddy Engineering College (Autonomous), Hyderabad, Telangana, India.

sarada.chakireddy@gmail.com

Associate Professor, Avanathi Institute of Engineering and Technology, Hyderabad, Telangana, India.

pjravindranath@gmail.com

ABSTRACT *In this present study, we consider an incompressible heat and mass transfer with thermal radiation analysis for MHD peristaltic blood flow of a prandtl fluid under the influence of porous medium through a vertical tapered asymmetric channel. The gravity field is taken into the account. The left wall of the channel is maintained at temperature T_0 , whereas the right wall has temperature T_1 . The right and left wall boundaries of the tapered asymmetric channel are $Y = H_1$ and $Y = H_2$. We tend to assume that the fluid is subject to a relentless transverse magnetic field B_0 . The fluid is induced by sinusoidal wave trains propagating with constant speed c along the channel walls.*

KEY WORDS: *Heat and mass transfer, Peristaltic Fluid Flow, porous channel, thermal radiation.*

I. INTRODUCTION

Past few years, a good variety of scholars consummates blood flow through various channels. The Literature of Biomathematics has provided with the vast variety of applications in drugs and biology. Peristalsis has its monumental applications in the medical physiology. In medical physiology, it's concerned with the motion of food material within the disagreeable person, as an example, within the propulsion of food bolus within the passage, conversion of food bolus into nutrient within the abdomen and movement of nutrient within the bowel. Peristaltic motion in the industrial applications is engaged in the transport of corrosive and noxious fluids, roller and finger pumps, hose pumps, tube pumps, dialysis machines and heart-lung machines. Latham [1] and Shapiro et al. [2] conferred the peristalsis of viscous fluids through theoretical and experimental approaches. Parkes and Burns [3] have studied the peristaltic flow produced by sinusoidal peristaltic wave along a flexible wall of the channel under the pressure gradient. After these studies, several investigators Fung and Yih [4], Zien and Ostrach [5], Raju and Devanathan [6], Srivastava et al. [7], Xiao and Damodaran [8], Elshehawey and Sobh [9], Umavathi et al. [10], Radhakrishnamacharya and Srinivasulu [11], Kalidas Das [12], Lika Hummady et al. [13], Ravikumar [14 and 15] and Kothandapani et al. [16] have studied peristaltic problems under various assumptions. Gangavathi et al. [17] have scrutinized the peristaltic flow of a prandtl fluid in an asymmetric channel under the effect of magnetic field. In another paper, Noreen Sher Akbar et al. [18] found that the peristaltic flow of a prandtl fluid model in an asymmetric channel. Kumar et al. [19] have analysed an influence of velocity slip conditions on MHD peristaltic flow of a prandtl fluid in a non-uniform channel. Nadeem et al. [20] studied the series solution of three-dimensional peristaltic flow of Prandtl fluid in a rectangular channel. Rahmat Ellahi and Arshad Riaz [21] have presented a theory on peristaltic flow of a prandtl fluid model in an asymmetric. Convective heat transfer analysis on prandtl fluid model with peristalsis by Alsaedi et al. [22]. Sivaiah and Hemadri Reddy [23] investigated an effect of slip conditions on the peristaltic transport of a conducting prandtl fluid in a porous non-uniform channel. Nadeem et al. [24] carried out the peristaltic flow for a Prandtl fluid model in an endoscope.

Heat and mass transfer plays a significant role in body process attributable to its intensive applications in engineering and biomechanics. Further, the biological connection of heat transfer with peristalsis can be seen within the process of oxygenation and hemodialysis. Though of the field in peristaltic flows gained the abundant interest of researchers with respect to the issues involving physiological fluids as blood. Having such preference in mind, some authors (Ogulu [25], Eldabe [26], Srinivas and Kothandapani [27],FAbbasi [28], Ravikumar [29], Abd-Alla et al. [30],Hayat [31],Ramesh [32],Sheikholeslami et al.[33],Ravi Kumar and Ameer Ahamad [34],Abbasi, Shehzad [35]) analyzed the peristaltic transport with heat transfer and mass transfer.

2. FORMULATION OF THE PROBLEM

In this present study, we consider an incompressible heat and mass transfer with thermal radiation analysis for MHD peristaltic blood flow of a prandtlfluid under the influence of porous medium through a vertical tapered asymmetric channel. The gravity field is taken into the account.The left wall of the channel is maintained at temperature T_0 , whereas the right wall has temperature T_1 . The right and left wall boundaries of the tapered asymmetric channel are $Y = H_1$ and $Y = H_2$.We tend to assume that the fluid is subject to a relentless transverse magnetic field B_0 . The fluid is induced by sinusoidal wave trains propagating with constant speed c along the channel walls.

The geometry of the wall deformations are drawn by the subsequent expressions

$$y = H_2 = b + m'x + d \sin \left[\frac{2\pi}{\lambda} (x - ct) \right] \quad (2.1)$$

$$y = H_1 = -b - m'x - d \sin \left[\frac{2\pi}{\lambda} (x - ct) + \phi \right] \quad (2.2)$$

Where b is the half-width of the channel, d is the wave amplitude, c is the phase speed of the wave and m' ($m' \ll 1$) is the non-uniform parameter, λ is the wavelength, t is the time and X are the directions of wave propagation. The phase difference ϕ varies in the range $0 \leq \phi \leq \pi$, $\phi = 0$ corresponds to the symmetric channel with waves out of phase and further b, d and ϕ satisfy the following conditions for the divergent channel at the inlet $d \cos \left(\frac{\phi}{2} \right) \leq b$.

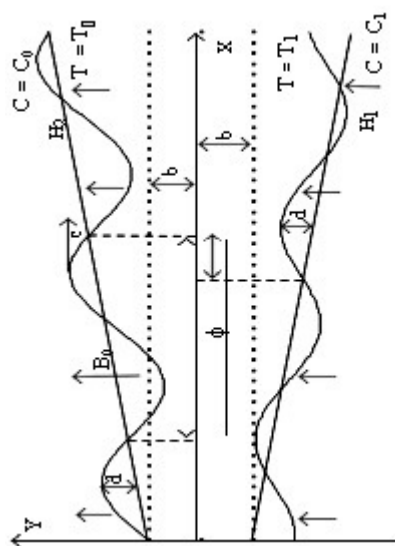


Fig. 1 Schematic diagram of the physical model

The equations governing the motion for the present problem prescribed by

The continuity equation is

$$\frac{\partial u}{\partial x} + \frac{\partial v}{\partial y} = 0(2.3)$$

The momentum equations are

$$\rho \left[u \frac{\partial u}{\partial x} + v \frac{\partial u}{\partial y} \right] = - \frac{\partial p}{\partial x} + \frac{\partial}{\partial x} \tau_{xx} + \frac{\partial}{\partial y} \tau_{xy} - \sigma B_0^2 (u + c) - \frac{\mu}{k_1} (u + c) + \rho g \sin \alpha(2.4)$$

$$\rho \left[u \frac{\partial v}{\partial x} + v \frac{\partial v}{\partial y} \right] = - \frac{\partial p}{\partial y} + \frac{\partial}{\partial x} \tau_{yx} + \frac{\partial}{\partial y} \tau_{yy} - \rho g \cos \alpha(2.5)$$

The energy equation is

$$\rho C_p \left[u \frac{\partial T}{\partial x} + v \frac{\partial T}{\partial y} \right] = k \left[\frac{\partial^2 T}{\partial x^2} + \frac{\partial^2 T}{\partial y^2} \right] + Q_0 + \sigma B_0^2 u^2 - \frac{\partial q_r}{\partial y} \tag{2.6}$$

The Concentration equation is

$$\left[u \frac{\partial C}{\partial x} + v \frac{\partial C}{\partial y} \right] T = D_m \left[\frac{\partial^2 C}{\partial x^2} + \frac{\partial^2 C}{\partial y^2} \right] \frac{D_m K_T}{T_m} \left[\frac{\partial^2 T}{\partial x^2} + \frac{\partial^2 T}{\partial y^2} \right] \tag{2.7}$$

u and v are the velocity components in the corresponding coordinates, k_1 is the permeability of the porous medium, ρ is the density of the fluid, p is the fluid pressure, μ is the coefficient of the viscosity, σ is the electrical conductivity, g is the acceleration due to gravity, Q_0 is the constant heat addition/absorption, C_p is the specific heat at constant pressure, D_m is the coefficient of mass diffusivity, T_m is the mean temperature, K_T is the thermal diffusion ratio T is the temperature of the fluid and q_r is the radioactive heat flux.

Hence, for the Rosseland approximation for thermal radiation, we have

$$q_r = - \frac{16 \sigma^* T_0^3}{3k^*} \frac{\partial T}{\partial y}$$

where σ^* and k^* are the Stefan-Boltzmann constant and the mean absorption coefficient.

The Constitutive equations for Prandtl fluid is given by (Patel and Timaol [36])

$$\tau = \left[\frac{A \sin^{-1} \left[\frac{1}{c} \left(\frac{\partial u}{\partial y} \right)^2 + \left(\frac{\partial v}{\partial x} \right)^2 \right]^{\frac{1}{2}}}{\left[\left(\frac{\partial u}{\partial y} \right)^2 + \left(\frac{\partial v}{\partial x} \right)^2 \right]^{\frac{1}{2}}} \right] \frac{\partial u}{\partial y}$$

Where A and C are material constants of prandtl fluid model.

Introducing the following non-dimensional quantities:

$$\bar{x} = \frac{x}{\lambda} \bar{y} = \frac{y}{b} \bar{t} = \frac{ct}{\lambda} \bar{u} = \frac{u}{c} \bar{v} = \frac{v}{c\delta} h_1 = \frac{H_1}{b} h_2 = \frac{H_2}{b} \bar{p} = \frac{b^2 p}{c\lambda\mu} Da = \frac{k_1}{b^2} \delta = \frac{b}{\lambda} Re = \frac{\rho cb}{\mu} M = B_0 b \sqrt{\frac{\sigma}{\mu}} Pr =$$

$$\frac{\mu C_p}{\kappa} \nu = \frac{Q_0 b^2}{\mu C_p (T_1 - T_0)} \varepsilon = \frac{d}{b} \theta = \frac{\bar{T} - T_0}{T_1 - T_0} \Phi = \frac{C - C_0}{C_1 - C_0} \eta = \frac{\rho a_0^2 g}{\mu c} \eta_1 = \frac{\rho a_0^3 g}{\lambda \mu c} S_c = \frac{\mu}{D_m \rho},$$

$$S_r = \frac{D_m \rho k_T (T_1 - T_0)}{\mu T_m (C_1 - C_0)} R_n = \frac{16 \sigma^* T_0^3 b^2}{3k^* \mu C_p} \tag{2. 8}$$

where $\varepsilon = \frac{d}{b}$ is the non-dimensional amplitude of channel, $\delta = \frac{b}{\lambda}$ is the wave number, $k_1 = \frac{\lambda m'}{b}$ is the

non - uniform parameter, Re is the Reynolds number, Da is the porosity parameter, M is the Hartman

number, ν is the heat source/sink parameter, R_n is the thermal radiation parameter, η and η_1 are gravitational parameters, Pr is the prandtl number S_c Schmidt number and S_r Soret number.

Now using non-dimensional quantities in equations (2.3-2.7) are reduced to the following non-dimensional form after dropping the bars,

$$Re\delta \left[u \frac{\partial u}{\partial x} + v \frac{\partial u}{\partial y} \right] = -\frac{\partial p}{\partial x} + \frac{\partial}{\partial y} \tau_{yx} + \delta \frac{\partial}{\partial x} \tau_{xx} - \left(M^2 + \frac{1}{Da} \right) u - \left(M^2 + \frac{1}{Da} \right) + \eta \sin \alpha \quad (2.9)$$

$$Re\delta \left[u \frac{\partial v}{\partial x} + v \frac{\partial v}{\partial y} \right] = -\frac{\partial p}{\partial y} + \delta^2 \frac{\partial}{\partial y} \tau_{xy} + \delta \frac{\partial}{\partial y} \tau_{yy} - \eta_1 \cos \alpha \quad (2.10)$$

$$Re \left[\delta u \frac{\partial \theta}{\partial x} + v \frac{\partial \theta}{\partial y} \right] = \frac{1}{Pr} \left[\delta^2 \frac{\partial^2 \theta}{\partial x^2} + \frac{\partial^2 \theta}{\partial y^2} \right] + \beta + R_n \frac{\partial^2 \theta}{\partial y^2} \quad (2.11)$$

$$Re\delta \left[u \frac{\partial \phi}{\partial x} + v \frac{\partial \phi}{\partial y} \right] = \frac{1}{S_c} \left[\delta^2 \frac{\partial^2 \phi}{\partial x^2} + \frac{\partial^2 \phi}{\partial y^2} \right] + \frac{1}{S_r} \left[\delta^2 \frac{\partial^2 \phi}{\partial x^2} + \frac{\partial^2 \phi}{\partial y^2} \right] \quad (2.12)$$

Applying long wavelength approximation and neglecting the wave number along with low-Reynolds numbers. Equations (2.9 - 2.12) become

$$\frac{\partial p}{\partial x} = \frac{\partial}{\partial y} \tau_{yx} - \left(M^2 + \frac{1}{Da} \right) u - \left(M^2 + \frac{1}{Da} \right) + \eta \sin \alpha \quad (2.13)$$

$$\frac{\partial p}{\partial y} = 0 \quad (2.14)$$

$$\frac{1}{Pr} \frac{\partial^2 \theta}{\partial y^2} + \nu + R_n \frac{\partial^2 \theta}{\partial y^2} = 0 \quad (2.15)$$

$$\frac{1}{S_c} \frac{\partial^2 \phi}{\partial y^2} + S_r \frac{\partial^2 \phi}{\partial y^2} = 0 \quad (2.16)$$

here

$$\tau_{yx} = \alpha \left(\frac{\partial u}{\partial y} \right) + \frac{\beta}{6} \left(\frac{\partial u}{\partial y} \right)^3, \text{ where } \alpha \text{ and } \beta \text{ are Prandtl fluid parameters}$$

The relative boundary conditions in dimensionless form are given by

$$u = -1, \theta = 0, \phi = 0 \text{ at } y = h_1 = 1 - k_1 x - \varepsilon \sin[2\pi(x - t) + \phi] \quad (2.17)$$

$$u = -1, \theta = 0, \phi = 0 \text{ at } y = h_2 = 1 + k_1 x + \varepsilon \sin[2\pi(x - t)] \quad (2.18)$$

Equation (2.14) indicates that p is independent of y . Therefore, equation (2.13) can be rewritten as

$$\frac{\partial p}{\partial x} = \frac{\partial}{\partial y} \left(\alpha \left(\frac{\partial u}{\partial y} \right) + \frac{\beta}{6} \left(\frac{\partial u}{\partial y} \right)^3 \right) - \left(M^2 + \frac{1}{Da} \right) u - \left(M^2 + \frac{1}{Da} \right) + \eta \sin \alpha \quad (2.19)$$

The volumetric flow rate in the wave frame is defined by

$$q = \int_{h_1}^{h_2} u \, dy \quad (2.20)$$

The instantaneous flux $Q(x, t)$ in the laboratory frame is

$$Q = \int_{h_2}^{h_1} (u + 1) \, dy = q + (h_1 - h_2) \quad (2.21)$$

The average volume flow rate over one wave period ($T = \lambda/c$) of the peristaltic wave is defined as

$$\bar{Q} = \frac{1}{T} \int_0^T Q \, dt = q + 1 + d \quad (2.22)$$

3. SOLUTION OF THE PROBLEM

Equation 2.19 is a non-linear equation and it's difficult to induce a closed type answer. But for vanishing β , the boundary value problem is agreeable to a simple analytical answer. Throughout this case,

the equation becomes linear and should be solved. Thus we have a tendency to expand the flow quantities during a series of the little parameter prandtl number β as follows.

$$\left. \begin{aligned} u &= u_0 + \beta u_1 + O(\beta^2) \\ \frac{\partial p}{\partial x} &= \frac{\partial p_0}{\partial x} + \beta \frac{\partial p_1}{\partial x} + O(\beta^2) \\ q &= q_0 + \beta q_1 + O(\beta^2) \end{aligned} \right\} \tag{3.1}$$

Substituting (3.1) in the equation (2.19) and the boundary conditions (2.17) and (2.18) and equating the coefficients of like powers of β , we get

3.1 System of order zero (β^0)

$$\alpha \frac{\partial^2 u_0}{\partial y^2} - \left(M^2 + \frac{1}{Da}\right) u_0 = \frac{\partial p_0}{\partial x} + \left(M^2 + \frac{1}{Da}\right) - \eta \sin \alpha \tag{3.2}$$

The relative boundary conditions in dimensionless form are given by

$$u_0 = -1 \text{ at } y = h_1 = 1 - k_1 x - \varepsilon \sin[2\pi(x - t) + \phi] \tag{3.3}$$

$$u_0 = -1 \text{ at } y = h_2 = 1 + k_1 x + \varepsilon \sin[2\pi(x - t)] \tag{3.4}$$

Solving equation (3.2) together with the boundary conditions (3.3) and (3.4), we obtain

$$u_0 = C \sinh[\sqrt{A}y] + D \cosh[\sqrt{A}y] - \left[\frac{p_0}{A\alpha}\right] - B \tag{3.5}$$

Where

$$\begin{aligned} A &= \frac{\left(M^2 + \frac{1}{Da}\right)}{\alpha} B = 1 - \frac{1}{A\alpha} \eta \sin \alpha C = \left[\frac{a_2 - \left[\frac{p_0}{A\alpha}\right] a_2 - B a_2}{a_1} \right] D \\ &= \left[\frac{-1 + B + \left[\frac{p_0}{A\alpha}\right] - C \sinh[\sqrt{A}h_1]}{\cosh[\sqrt{A}h_1]} \right] p_0 = \frac{\partial p_0}{\partial x} a_1 \\ &= \left[\frac{\sinh[\sqrt{A}h_1] \cos[\sqrt{A}h_2] - \sinh[\sqrt{A}h_2] \cos[\sqrt{A}h_1]}{a_2 = [\cos[\sqrt{A}h_1] - \cos[\sqrt{A}h_2]]} \right] \end{aligned}$$

The volumetric flow rate q_0 in the moving coordinate system is given by

$$q_0 = \int_{h_1}^{h_2} u_0 dy = \int_{h_1}^{h_2} \left(C \sinh[\sqrt{A}y] + D \cosh[\sqrt{A}y] - \left[\frac{p_0}{A\alpha}\right] - B \right) dy = p_0 a_5 + a_6 \tag{3.6}$$

From the equation (3.6), $\frac{\partial p_0}{\partial x}$ can be expressed as

$$\frac{\partial p_0}{\partial x} = \frac{q_0 - a_6}{a_5} \tag{3.7}$$

$$\begin{aligned} a_3 &= \sinh[\sqrt{A}h_2] - \sinh[\sqrt{A}h_1] a_4 = \cosh[\sqrt{A}h_2] - \cosh[\sqrt{A}h_1] \\ a_5 &= \frac{a_3}{\sqrt{A} A \alpha \cos[\sqrt{A}h_1]} + \frac{a_2 a_3 \sinh[\sqrt{A}h_1]}{\sqrt{A} A \alpha a_1 \cos[\sqrt{A}h_1]} - \frac{a_2 a_4}{\sqrt{A} A \alpha a_1} - \frac{(h_2 - h_1)}{A \alpha} \\ a_6 &= \frac{-a_3 \eta \sin \alpha}{\sqrt{A} A \alpha \cos[\sqrt{A}h_1]} - \frac{a_2 a_3 \eta \sin \alpha \sinh[\sqrt{A}h_1]}{\sqrt{A} A \alpha a_1 \cos[\sqrt{A}h_1]} + \frac{a_2 a_4 \eta \sin \alpha}{\sqrt{A} A \alpha a_1} + \frac{(h_2 - h_1) \eta \sin \alpha}{A \alpha} \\ &\quad - (h_2 - h_1) \end{aligned}$$

3.2 System of first order (β)

$$\alpha \frac{\partial^2 u_1}{\partial y^2} - \left(M^2 + \frac{1}{Da}\right) u_1 = \frac{\partial p_1}{\partial x} - \frac{1}{6} \frac{\partial}{\partial y} \left(\frac{\partial u_0}{\partial y}\right)^3 \tag{3.8}$$

The relative boundary conditions in dimensionless form are given by

$$u_1 = 0 \text{ at } y=h_1 = 1 - k_1 x - \varepsilon \sin[2\pi(x - t) + \phi] \tag{3.9}$$

$$u_1 = 0 \text{ at } y=h_2 = 1 + k_1 x + \varepsilon \sin[2\pi(x - t)] \tag{3.10}$$

Solving equation (3.8) together with the boundary conditions (3.9) and (3.10), we obtain

$$u_1 = (f_{11} b_1 + f_{17}) \cosh[\sqrt{A}y] + (f_{11} b + f_{16}) \sinh[\sqrt{A}y] - f_{11} - f_{12} e^{3\sqrt{A}y} + f_{13} e^{-3\sqrt{A}y} - f_{14} y e^{\sqrt{A}y} - f_{15} y e^{-\sqrt{A}y} \tag{3.11}$$

$$b = a_4 = \cosh[\sqrt{A}h_2] - \cosh[\sqrt{A}h_1] b_1 = \left[\frac{1 - b \sinh[\sqrt{A}h_1]}{\cosh[\sqrt{A}h_1]} \right] f_1 = D\sqrt{A}f_2 = C\sqrt{A}$$

$$f_3 = \left(\frac{f_1^3}{8} + \frac{f_2^3}{8} + \frac{3f_1^2 f_2}{8} + \frac{3f_2^2 f_1}{8} \right) f_4 = \left(-\frac{f_1^3}{8} + \frac{f_2^3}{8} + \frac{3f_1^2 f_2}{8} - \frac{3f_2^2 f_1}{8} \right)$$

$$f_5 = \left(-\frac{f_1^3}{8} + \frac{f_2^3}{8} - \frac{3f_1^2 f_2}{8} + \frac{3f_2^2 f_1}{8} \right) f_6 = \left(\frac{f_1^3}{8} + \frac{f_2^3}{8} - \frac{3f_1^2 f_2}{8} - \frac{3f_2^2 f_1}{8} \right) f_7 = \frac{3\sqrt{A}f_3}{6\alpha} f_8 = \frac{3\sqrt{A}f_4}{6\alpha} f_9$$

$$= \frac{\sqrt{A}f_5}{6\alpha} f_{10} = \frac{\sqrt{A}f_6}{6\alpha} f_{11} = \frac{p_1}{A\alpha} f_{12} = \frac{f_7}{8A} f_{13} = \frac{f_8}{8A} f_{14} = \frac{f_9}{2\sqrt{A}} f_{15} = \frac{f_{10}}{2\sqrt{A}}$$

$$f_{16} = \frac{f_{12} \left(\cosh[\sqrt{A}h_2] e^{3\sqrt{A}h_1} - \cosh[\sqrt{A}h_1] e^{3\sqrt{A}h_2} \right)}{\left[\sinh[\sqrt{A}h_1] \cos[\sqrt{A}h_2] - \sinh[\sqrt{A}h_2] \cos[\sqrt{A}h_1] \right]}$$

$$+ \frac{f_{13} \left(\cosh[\sqrt{A}h_1] e^{-3\sqrt{A}h_2} - \cosh[\sqrt{A}h_2] e^{3\sqrt{A}h_1} \right)}{\left[\sinh[\sqrt{A}h_1] \cos[\sqrt{A}h_2] - \sinh[\sqrt{A}h_2] \cos[\sqrt{A}h_1] \right]}$$

$$+ \frac{f_{14} \left(h_1 \cosh[\sqrt{A}h_2] e^{\sqrt{A}h_1} - h_2 \cosh[\sqrt{A}h_1] e^{\sqrt{A}h_2} \right)}{\left[\sinh[\sqrt{A}h_1] \cos[\sqrt{A}h_2] - \sinh[\sqrt{A}h_2] \cos[\sqrt{A}h_1] \right]}$$

$$+ \frac{f_{15} \left(h_1 \cosh[\sqrt{A}h_2] e^{-\sqrt{A}h_1} - h_2 \cosh[\sqrt{A}h_1] e^{-\sqrt{A}h_2} \right)}{\left[\sinh[\sqrt{A}h_1] \cos[\sqrt{A}h_2] - \sinh[\sqrt{A}h_2] \cos[\sqrt{A}h_1] \right]}$$

$$f_{17} = \frac{f_{12} e^{3\sqrt{A}h_1} - f_{13} e^{-3\sqrt{A}h_1} + f_{14} h_1 e^{\sqrt{A}h_1} + f_{15} h_1 e^{-\sqrt{A}h_1} - f_{16} \sinh[\sqrt{A}h_1]}{\cosh[\sqrt{A}h_1]}$$

The volume flow rate q_1 in the moving coordinate system is given by

$$q_1 = \int_{h_1}^{h_2} u_1 dy = f_{11} f_{19} + f_{20} \tag{3.12}$$

the equation (3.12), $\frac{\partial p_1}{\partial x}$ can be expressed as

$$\frac{\partial p_1}{\partial x} = \frac{(q_1 - f_{20}) A \alpha}{f_{19}} \tag{3.13}$$

$$f_{19} = \frac{b_1}{\sqrt{A}} \left(\sinh[\sqrt{A}h_2] - \sinh[\sqrt{A}h_1] \right) + \frac{b}{\sqrt{A}} \left(\cosh[\sqrt{A}h_2] - \cosh[\sqrt{A}h_1] \right) - (h_2 - h_1)$$

$$\begin{aligned}
 f_{20} = & \frac{f_{17}}{\sqrt{A}} (\sinh[\sqrt{A}h_2] - \sinh[\sqrt{A}h_1]) + \frac{f_{16}}{\sqrt{A}} (\cosh[\sqrt{A}h_2] - \cosh[\sqrt{A}h_1]) \\
 & - \frac{f_{12}}{3\sqrt{A}} (e^{3\sqrt{A}h_2} - e^{3\sqrt{A}h_1}) + \frac{f_{13}}{3\sqrt{A}} (e^{-3\sqrt{A}h_1} - e^{-3\sqrt{A}h_2}) \\
 & - f_{14} \left(\left(\frac{h_2 e^{\sqrt{A}h_2}}{\sqrt{A}} - \frac{e^{\sqrt{A}h_2}}{A} \right) - \left(\frac{h_1 e^{\sqrt{A}h_1}}{\sqrt{A}} - \frac{e^{\sqrt{A}h_1}}{A} \right) \right) \\
 & - f_{15} \left(\left(\frac{-h_2 e^{-\sqrt{A}h_2}}{\sqrt{A}} - \frac{e^{-\sqrt{A}h_2}}{A} \right) - \left(\frac{-h_1 e^{-\sqrt{A}h_1}}{\sqrt{A}} - \frac{e^{-\sqrt{A}h_1}}{A} \right) \right)
 \end{aligned}$$

The dimensionless pressure rise per one wavelength in the wave frame is defined as

$$\Delta p = \int_0^1 \frac{dp}{dx} dx \tag{3.14}$$

The dimensionless friction force F at the wall (right wall) across one wavelength is given by

$$F = \int_0^1 h_1^2 \left(-\frac{dp}{dx} \right) dx \tag{3.15}$$

The solutions of temperature and concentration with subject to boundary conditions (2.18) and (2.19) are given by

$$\theta = n_1 + n_2 y + \frac{E}{2} y^2 \tag{3.16}$$

$$\Phi = n_3 + n_4 y - \frac{S_c S_r E}{2} y^2 \tag{3.17}$$

Where

$$\begin{aligned}
 n_1 = & \frac{E h_1^2}{2} - \left(\frac{-1 - \frac{E}{2}(h_1^2 - h_2^2)}{h_1 - h_2} \right) \times h_1 n_1 = \left(\frac{-1 - \frac{E}{2}(h_1^2 - h_2^2)}{h_1 - h_2} \right) \\
 n_3 = & \frac{S_c S_r E h_1^2}{2} - \left(\frac{-1 - \frac{S_c S_r E}{2}(h_1^2 - h_2^2)}{h_1 - h_2} \right) \times h_1 n_4 = \left(\frac{-1 - \frac{S_c S_r E}{2}(h_1^2 - h_2^2)}{h_1 - h_2} \right) E = \frac{\nu p_r}{1 + R_n Pr}
 \end{aligned}$$

4. NUMERICAL RESULTS AND DISCUSSION OF THE PROBLEM

The main object of this investigation has been to study the heat and mass transfer with thermal radiation analysis for hydromagnetic (MHD) peristaltic hemodynamic (blood) prandtl fluid model with the porous medium through a tapered vertical asymmetric inclined channel. The analytical expressions for velocity distribution, pressure gradient, pressure rise, frictional force, and temperature and concentration distributions have been derived in the previous section. The numerical and computational results are discussed through the graphical illustration. **Mathematica** software is used to find out numerical results. Throughout the computations we fix $k_1 = 0.1$, $\epsilon = 0.2$, $t = 0.4$, $x = 0.6$, $\phi = \frac{\pi}{6}$, $Da = 0.1$, $M = 5$, $\beta = 0.2$, $\alpha = 1.5$, $\theta = \frac{\pi}{6}$, $\eta = 0.5$, $d = 1$, $\bar{Q} = 0.5$, $Pr = 2$, $Rn = 0.1$, $\nu = 0.5$, $Sc = 0.2$ and $Sr = 2$.

4.1 Velocity profile

Figure (2) shows the variation of axial velocity with y for different values of Hartmann number (M) with fixed other parameters. It is clear that the axial velocity decreases with an increase in Hartmann number (M = 4, 5, 6). Figure (3) displays the effect of prandtl fluid parameter α on axial velocity distribution. It can be concluded from this figure that the axial velocity reduces with increase in prandtl fluid parameter α ($\alpha = 1.5, 2, 2.5$). Figure(4) is drawn to review the impact of prandtl fluid parameter β on axial velocity (u) with fixed other parameters. It is realized that the results in axial velocity reduce by an increase in prandtl

fluid parameter β . Figure (5) describe the influence of porosity parameter (Da) on axial velocity (u). We observe from this figure that the axial velocity enhances with the increase in porosity parameter (Da). Figure (6) elucidates that the influence of the gravity parameter (η) on axial velocity (u) distribution. Indeed, the fluid of the axial velocity enhances with an increase in η .

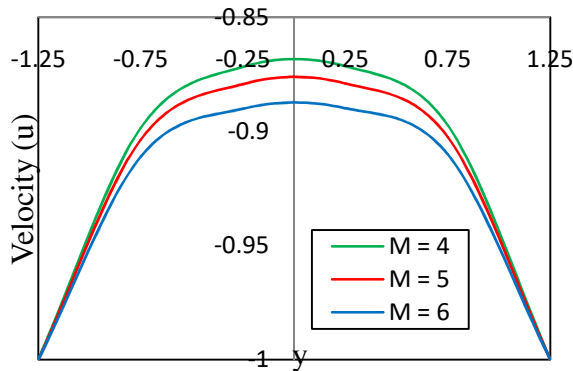


Fig.2 Impact of M on Axial velocity

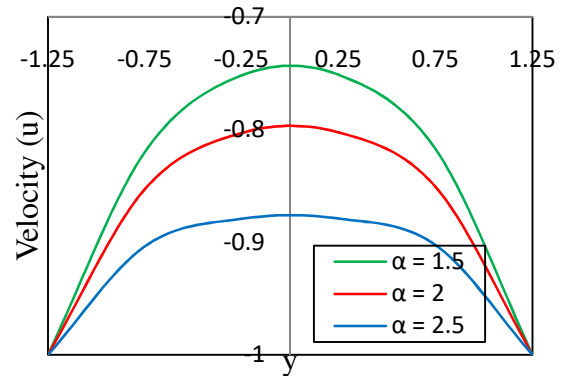


Fig.3 Impact of α on Axial velocity

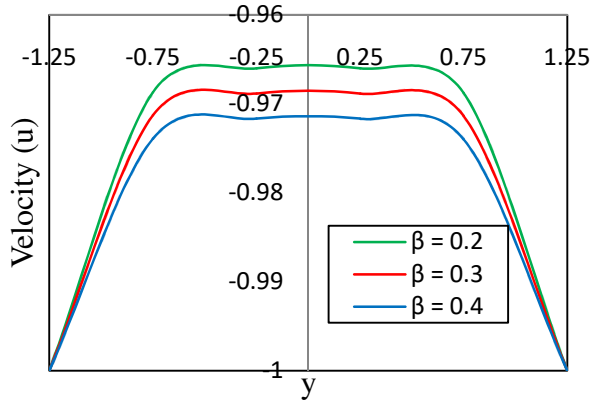


Fig.4 Impact of β on Axial velocity

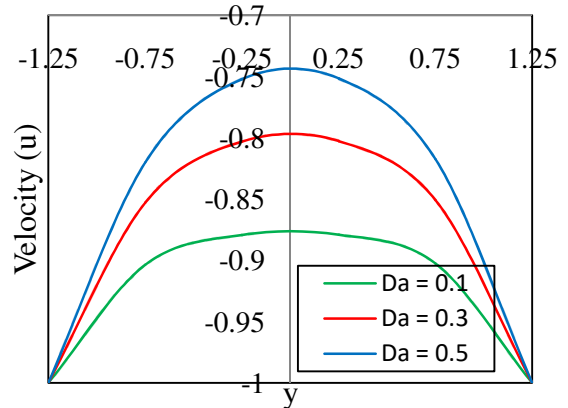


Fig.5 Impact of Da on Axial velocity

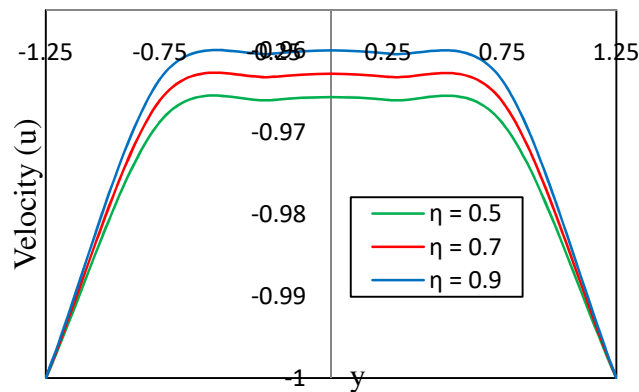


Fig.6 Impact of η on Axial velocity

Pumping characteristics

4.2 Pressure gradient

Pressure gradient has been calculated as a function of x from the equations (3.7 and 3.13) and plotted from the figures 7-10. Figure (7) represents the variation of the axial pressure gradient with x for different

values of Hartmann number (M). We notice from this figure that the pressure gradient increases in the wider part of the channel i.e. $x \in [0, 0.4] \cup [0.8, 1]$ while it reduces in the narrow part of the channel i.e. $x \in [0.4, 0.8]$ by an increase in Hartmann number ($M = 4, 5, 6$). However, the blood flow fluid cannot pass easily in the wider part of the channel, in this case, we need more pressure gradient to maintain the same flux to pass through it. Figure 8 is drawn to study the effect of volumetric flow rate (\bar{Q}) on pressure gradient. It can be seen that the pressure gradient enhances in the region $x \in [0.5, 0.75]$ while it reduces in other portion of the region $x \in [0.05, 0.5] \cup [0.75, 1]$. Therefore, we conclude from this figure that in the narrow part of the channel i.e. $x \in [0.5, 0.75]$, the blood flow cannot pass easily, we require large pressure gradient to maintain same flux to pass through it while in the wider part of the channel i.e. $x \in [0.05, 0.5] \cup [0.75, 1]$, the flow can easily pass without imposing large pressure gradient. The effect of Prandtl fluid parameter (α) on temperature profile is depicted in figure (9). We examine that the pressure gradient enhances near the boundary of the walls and also in $x \in [0.5, 0.8]$ and also we notice that the pressure gradient is maximum at $x = 0.6$, in case we require more pressure gradient to maintain the same flux to pass through it by an increase in prandtl fluid parameter α . An effect of prandtl fluid parameter (β) on axial pressure gradient is presented in figure (10). It is interesting to note that the pressure gradient enhances throughout the region $x \in [0, 1]$ by an increase in β , this enhancement in the pressure gradient due to the increment of prandtl fluid parameter (β). Therefore, the blood flow cannot pass easily in the entire tapered asymmetric channel, we require more pressure gradient to maintain the same flux through pass it.

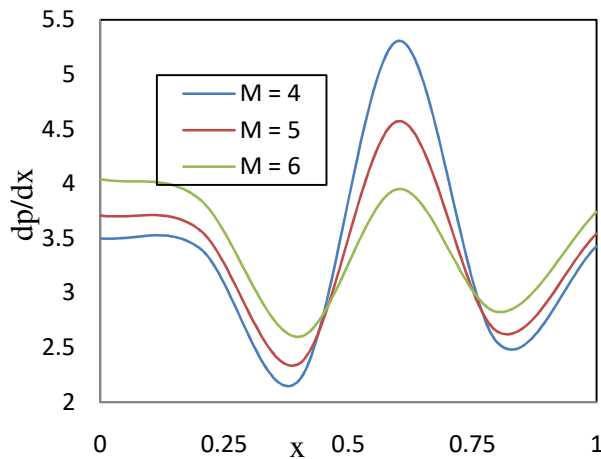


Fig.7 Impact of M on Pressure Gradient

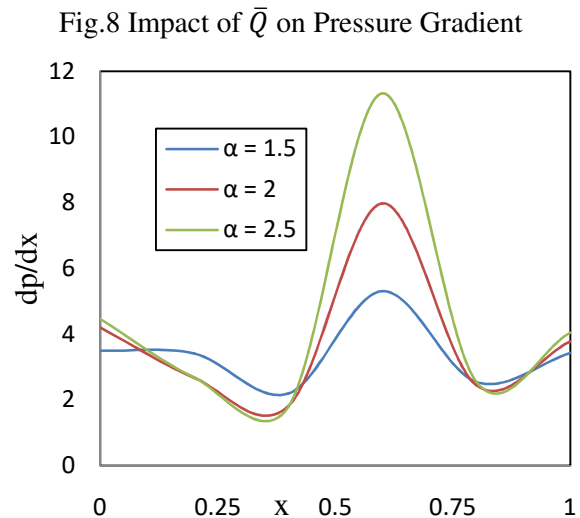
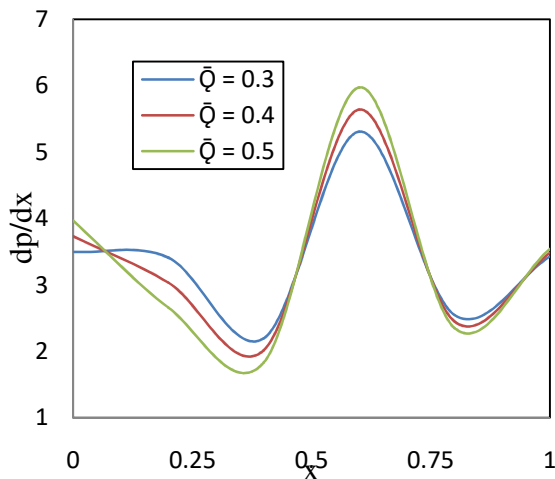
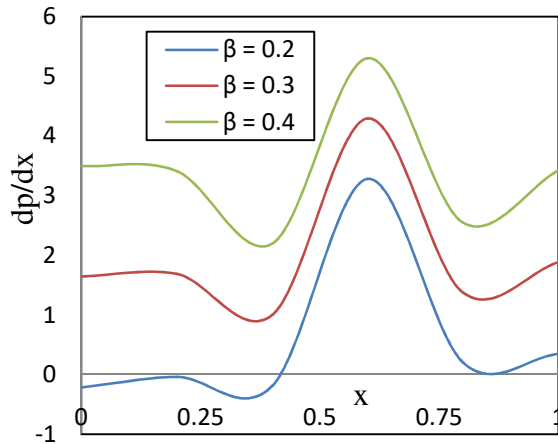


Fig.9 Impact of α on Pressure Gradient



Fig.10 Impact of β on Pressure Gradient

4.3 Pressure rise

The pressure rise against the volume flow rate for various parameters of interest is illustrated in Figs. (11) to (14). In these figures the region is divided into four parts: Peristaltic pumping region ($\Delta p > 0, \bar{Q} > 0$), retrograde pumping region ($\Delta p > 0, \bar{Q} < 0$), augmented region ($\Delta p < 0, \bar{Q} > 0$) and free pumping region ($\Delta p = 0$). Figure (11) reveals that the pressure rise versus volumetric flow rate \bar{Q} . This graph shows that with increasing the Hartmann number, the pumping rate \bar{Q} enhances in the entire retrograde ($\Delta p > 0, \bar{Q} < 0$) and also in peristaltic pumping ($\Delta p > 0, \bar{Q} > 0$) zones while the pumping rate gradually reduces in free pumping ($\Delta p = 0$) and co-pumping ($\Delta p < 0, \bar{Q} > 0$) zones. The effect of Prandtl fluid parameter (α) on pressure rise (Δp) is depicted in figure (12). It is interesting to note that the pumping rate rises in all four regions, i.e. retrograde pumping region ($\Delta p > 0, \bar{Q} < 0$), Peristaltic pumping region ($\Delta p > 0, \bar{Q} > 0$), free pumping region ($\Delta p = 0$) and an augmented region ($\Delta p < 0, \bar{Q} > 0$) with an increase in Prandtl fluid parameter (α). Figure (13) presented the various values of Prandtl fluid parameter (β) on pressure rise (Δp). We observe from this graph that the pumping rate enhances in retrograde ($\Delta p > 0, \bar{Q} < 0$) and also in peristaltic pumping ($\Delta p > 0, \bar{Q} > 0$) zones but the volumetric flow rate gradually reduces in the co-pumping region ($\Delta p < 0, \bar{Q} > 0$) by an increase in Prandtl fluid parameter (β). Impact of porosity parameter (Da) on pressure rise (Δp) is plotted in figure (14). We notice from this graph that the pumping rate gradually reduces in the entire retrograde ($\Delta p > 0, \bar{Q} < 0$) and also in peristaltic pumping ($\Delta p > 0, \bar{Q} > 0$) zones whereas the behavior is opposite in co-pumping region and also we notice that the pumping curves coincide with free pumping zone.

4.4 Frictional force

Figures (15) to (18) describe the variation of frictional force F against the flow rate for different parameters of interest. The frictional forces exactly have an opposite behavior when compared to the pressure rise.

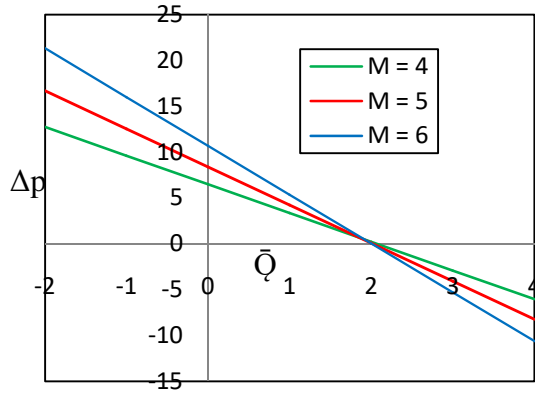


Fig.11 Impact of M on Pressure rise

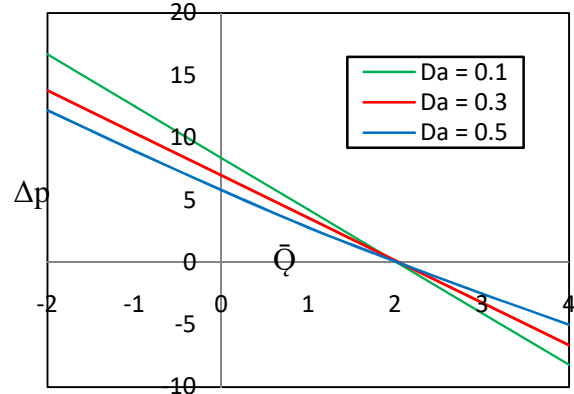


Fig.14 Impact of Da on Pressure rise

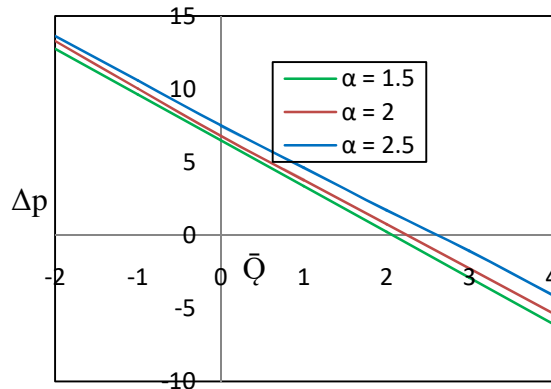


Fig.12 Impact of α on Pressure rise

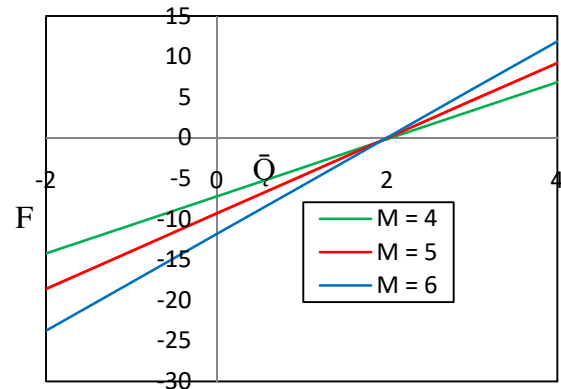


Fig.15 Impact of M on Friction force

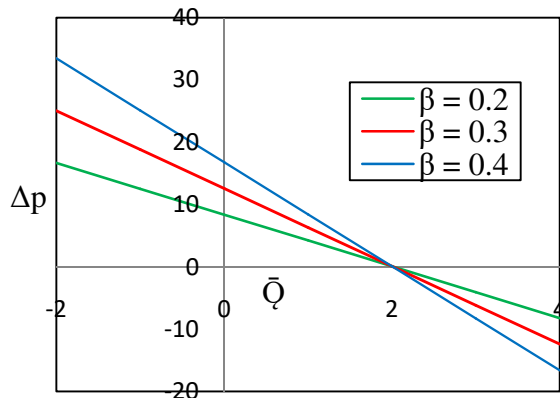


Fig.13 Impact of β on Pressure rise

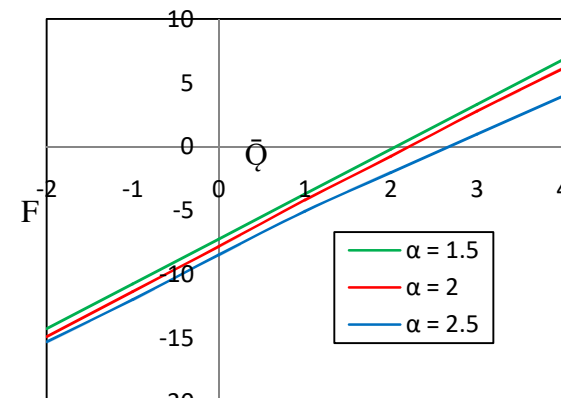


Fig.16 Impact of α on Friction force

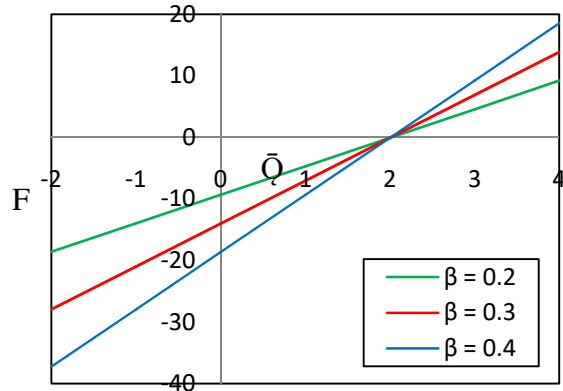


Fig.17 Impact of β on Friction force

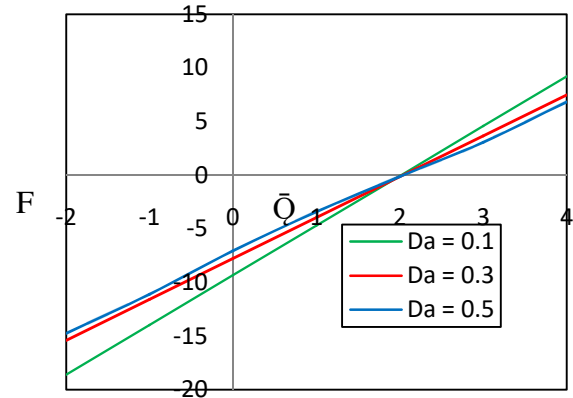


Fig.18 Impact of Da on Friction force

4.5 Heat transfer Analysis

Variations of temperature distribution (θ) with respect to y for various values of interest like thermal radiation parameter (Rn), prandtl number (Pr), heat source parameter (ν) and shifting operator (ϕ) are shown in figures 19 – 22. Figure 19 describes the behaviour of thermal radiation influence on temperature distribution. This graph shows that temperature of the fluid reduces within the tapered asymmetric vertical channel by an increase in thermal radiation parameter ($Rn = 0.1, 0.2, 0.3$) with fixed other parameters. Impact of prandtl number on temperature distribution is plotted in figure 20. This figure indicates that the results in the temperature of the fluid enhance with an increase in prandtl number ($Pr = 2, 5, 8$). Figure 21 is sketched for various values of heat source parameter (ν) over the temperature of the fluid. We notice from this figure that the temperature of the fluid increases with an increase in source parameter ($\nu = 0.1, 0.2, 0.3$). Figure (22) displays the variation in temperature of the fluid with the shift operator (ϕ). It is seen clearly from this figure that, as shift operator increases, temperature profile diminished within the tapered channel.

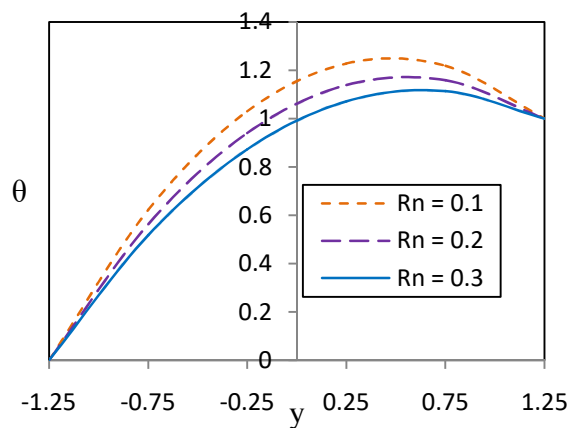


Fig.19 Impact of Rn on Temperature

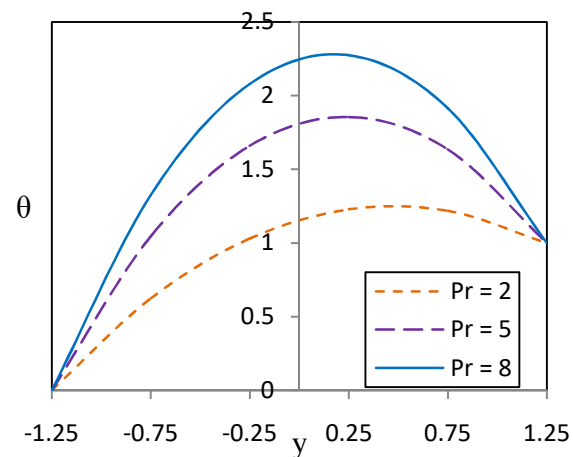


Fig.20 Impact of Pr on Temperature

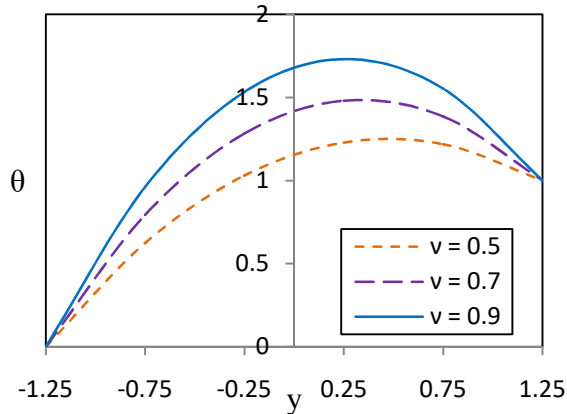


Fig.21 Impact of ν on Temperature

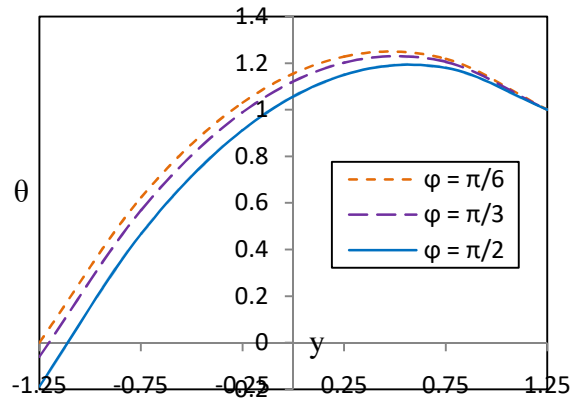


Fig.22 Impact of ϕ on Temperature

4.6 Mass transfer analysis

The influence of thermal radiation parameter (R_n), prandtl number (Pr), heat source/sink parameter (ν), schmidt number (Sc) and soret number (Sr) on concentration distribution are shown graphically in Figs 23-27. Fig. 23 illustrates the effect of thermal radiation parameter (R_n) on concentration profile. We perceive from this graph that the concentration profile increases with an increase in thermal radiation parameter ($R_n = 0.1, 0.2, 0.3$). Effect of Prandtl number (Pr), Heat source/sink parameter (ν), Schmidt number (Sc) and Soret number (Sr) on Concentration profiles are depicted in Figs 24-27. We notice from these graphs that the results in concentration profile decreases throughout the asymmetric tapered channel with the increase in prandtl number (Pr), heat source/sink parameter (ν), schmidt number (Sc) and soret number (Sr) with fixed other parameters.

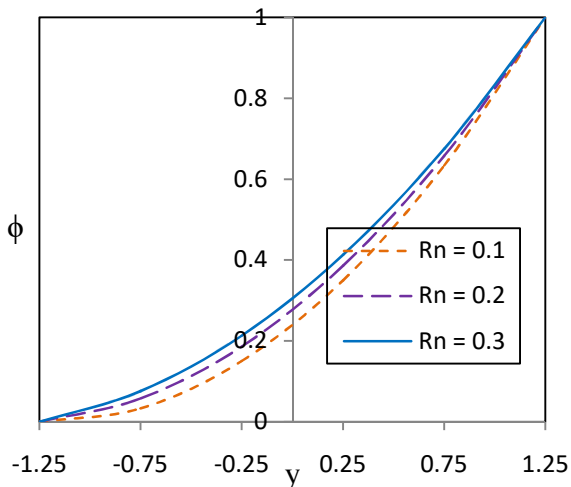


Fig.23 Impact of R_n on Concentration profile

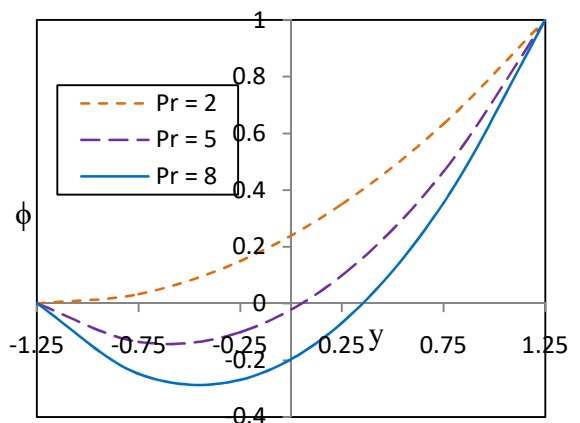


Fig.24 Impact of Pr on Concentration profile

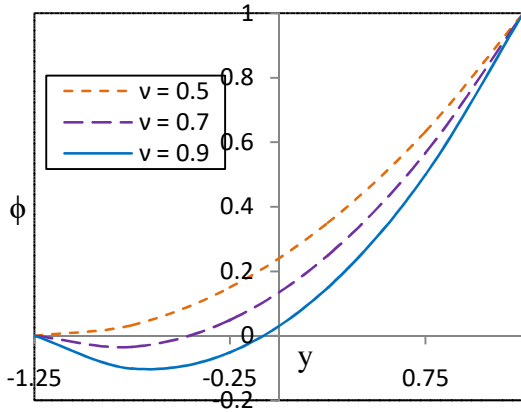


Fig.25 Impact of ν on Concentration profile

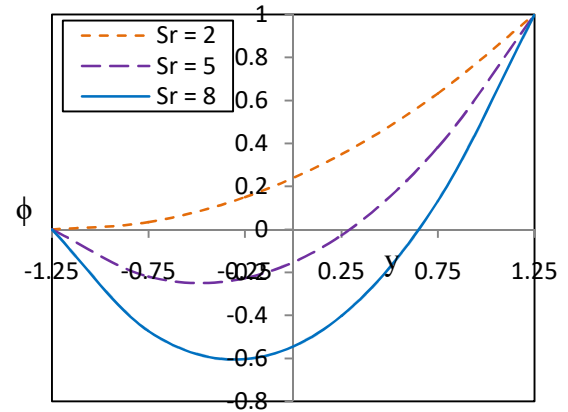


Fig.26 Impact of Sr on Concentration profile

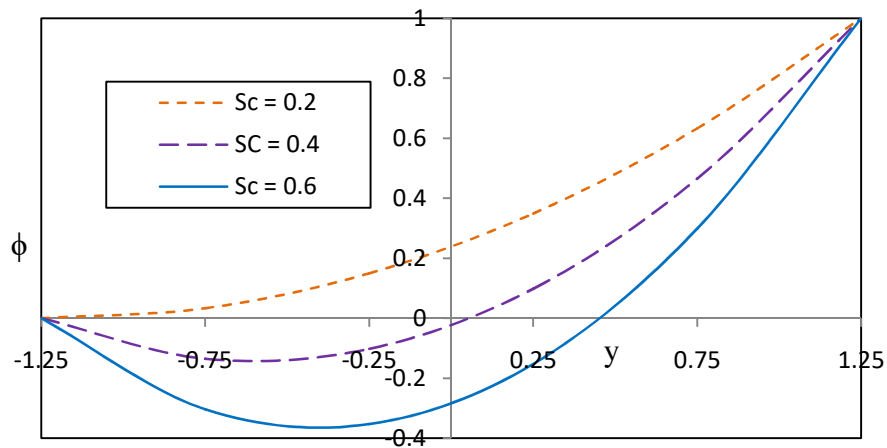


Fig.27 Impact of Sc on Concentration profile

5. CONCLUSIONS

Heat and mass transfer with thermal radiation analysis for hydromagnetic (MHD) peristaltic blood flow of a Prandtl fluid model with the porous medium through an asymmetric tapered vertical channel under the influence of gravity field has been investigated. The main findings are cited below.

- The axial velocity rises when rising in porosity parameter (Da) and gravitational parameter (η) while it reduces by an increase in hartmann number (M) and prandtl fluid parameters (α and β).
- The pressure gradient dp/dx enhances in the entire region $x \in [0, 1]$ by an increase in prandtl fluid parameters (β).
- Pumping rate enhances in retrograde ($\Delta p > 0, \bar{Q} < 0$) and also in peristaltic pumping ($\Delta p > 0, \bar{Q} > 0$) zones but the volumetric flow rate gradually reduces in the co-pumping region ($\Delta p < 0, \bar{Q} > 0$) by an increase in prandtl fluid parameter (β).
- Pumping rate rises in all the four regions, i.e. retrograde pumping region ($\Delta p > 0, \bar{Q} < 0$), Peristaltic pumping region ($\Delta p > 0, \bar{Q} > 0$), free pumping region ($\Delta p = 0$) and an augmented region ($\Delta p < 0, \bar{Q} > 0$) with the increase in prandtl fluid parameter (α).
- The frictional forces exactly have an opposite behavior when compared to the pressure rise.
- The temperature of the blood flow fluid rises with an increase in Pr and v while it reduces with increase in Rn and ϕ .
- The results in concentration distribution reduces with increase in Pr , v , Sr and Sc while it increases by increase in Rn .

NOMENCLATURE

u, v	velocity components (unit: m/s)	k^*	mean absorption coefficient
X, Y	cartesian coordinates	T, C	temperature (unit:K) and concentration
x, y	cartesian coordinates (unit: m)	k	thermal conductivity (uniy:W/(m.k))
b	width of the channel	k_1	permeability of the porous medium
d	wave amplitude (unit: m)	Q_0	heat addition/absorption
c	wave velocity (unit: m/s)	q_r	radioactive heat flux
g	acceleration due to gravity	C_p	specific heat at constant pressure
m'	non-uniform parameter	Re	reynolds number
t	time (unit:s)	\bar{Q}	volumetric flow rate (unit: m^3/s)
B_0	magnetic field (unit:T)	M	hartmann number
A, C	material constants of prandtl fluid model	Da	porosity parameter
T_0	left wall has temperature	Pr	prandtl number
T_1	right wall has temperature	Sc	schmidt number
p	fluid pressure	Sr	soret number
k^*	mean absorption coefficient	Rn	thermal radiation parameter

T, C	temperature (unit:K) and concentration	T_m D_m	mean temperature, mass diffusivity (unit: m^2/s)
F	friction force	K_T	thermal diffusion ratio

References

- [1] LATHAM T W. FLUID MOTION IN A PERISTALTIC PUMP. MS. THESIS 1966. MASSACHUSETTS INSTITUTE OF TECHNOLOGY, CAMBRIDGE, M.A.
- [2] SHAPIRO A H, JAFFRIN M Y AND WEINBERG S L. 1969. PERISTALTIC PUMPING WITH LONG WAVELENGTHS AT LOW REYNOLDS NUMBER. J. FLUID MECH.,37: 799-825.[HTTPS://DOI.ORG/10.1017/S0022112069000899](https://doi.org/10.1017/S0022112069000899)
- [3] PARKES J, BURNS J C. PERISTALTIC MOTION. J. FLUID MECHANICS1967: 29: 731–743.
I. DOI. [HTTPS://DOI.ORG/10.1017/S0022112067001156](https://doi.org/10.1017/S0022112067001156)
- [4] FUNG Y C, YIH C S. PERISTALTIC TRANSPORT. J. OF APPL. MECH., TRANS. ASME 1968: 5: 669-675.DOI. [HTTP://DX.DOI.ORG/10.1115/1.3601290](http://dx.doi.org/10.1115/1.3601290)
- [5] ZIEN T F, OSTRACH S A LONG WAVE LENGTH APPROXIMATION TO PERISTALTIC MOTION. J. OF BIOMECH.1970: 3: 63.DOI. [HTTP://DX.DOI.ORG/10.1016/0021-9290\(70\)90051-5](http://dx.doi.org/10.1016/0021-9290(70)90051-5)
- [6] RAJU KK, DEVANATHAN R.PERISTALTIC MOTION OF A NON-NEWTONIAN FLUID. RHEOL. ACTA.1972: 11: 170-179.
- [7] SRIVASTAVA L M, SRIVASTAVA V P, SINHA N S. PERISTALTIC TRANSPORT OF A PHYSIOLOGICAL FLUID, PART I, FLOW IN NON-UNIFORM GEOMETRY. BIORHEOLOGY 1983: 29:153-166.
II. DOI. [HTTP://DX.DOI.ORG/10.3233/BIR-1983-20205](http://dx.doi.org/10.3233/BIR-1983-20205)
- [8] XIAO Q, DAMODARAN M. A NUMERICAL INVESTIGATION OF PERISTALTIC WAVES IN CIRCULAR TUBES. INT. J. COMPUT. FLUID DYN. 2002:16: 201–216.
III. DOI. [HTTPS://DOI.ORG/10.1080/10618560290034681](https://doi.org/10.1080/10618560290034681)
- [9] ELSEHAWAY E F, SOBH A M. PERISTALTIC VISCOELASTIC FLUID MOTION IN A TUBE. INT. J. OF MATH.AND MATH, SCI. 2001:26:21-34.DOI. [HTTP://DX.DOI.ORG/10.1155/S0161171201003556](http://dx.doi.org/10.1155/S0161171201003556)
- [10] UMAVATHI J C, CHAMKHA A J, MANJULA M H, AL-MUDHAF A. FLOW AND HEAT TRANSFER OF A COUPLE-STRESS FLUID SANDWICHED BETWEEN VISCOUS FLUID LAYERS. J. OF PHYSICS 2005: 83 (7):705-720.[HTTPS://DOI.ORG/10.1139/p05-032](https://doi.org/10.1139/p05-032)
- [11] RADHAKRISHNAMACHARYA G, SRINIVASULU CH. INFLUENCE OF WALL PROPERTIES ON PERISTALTIC TRANSPORT WITH HEAT TRANSFER. COMPTES RENDUS MECHANIQUE 2007: 335: 369-373.
IV. DOI. [HTTPS://DOI.ORG/10.1016/J.CRME.2007.05.002](https://doi.org/10.1016/j.crme.2007.05.002)
- [12] KALIDAS DAS. EFFECTS OF SLIP AND HEAT TRANSFER ON MHD PERISTALTIC FLOW IN AN INCLINED ASYMMETRIC CHANNEL. IRANIAN JOURNAL OF MATHEMATICAL SCIENCES AND INFORMATICS 2012:7(2):35-52.DOI. [HTTPS://DOI.ORG/10.7508/IJMSI.2012.02.004](https://doi.org/10.7508/IJMSI.2012.02.004)
- [13] LIKA HUMMADY, AHMED ABDULHADI. INFLUENCE OF MHD ON PERISTALTIC FLOW OF COUPLE-STRESS FLUID THROUGH A POROUS MEDIUM WITH SLIP EFFECT. ADVANCES IN PHYSICS THEORIES AND APPLICATIONS 2014: 30: 34-44.
- [14] RAVIKUMAR S, EFFECT OF COUPLE STRESS FLUID FLOW ON MAGNETOHYDRODYNAMIC PERISTALTIC BLOOD FLOW WITH POROUS MEDIUM TROUGH INCLINED CHANNEL IN THE PRESENCE OF SLIP EFFECT-BLOOD FLOW STUDY.INTERNATIONAL JOURNAL OF BIO-SCIENCE AND BIO-TECHNOLOGY 2015:7(5):65-84.DOI.[HTTP://DX.DOI.ORG/10.14257/IJBSBT.2015.7.5.07](http://dx.doi.org/10.14257/IJBSBT.2015.7.5.07)
- [15] RAVIKUMAR S. EFFECTS OF THE COUPLE STRESS FLUID FLOW ON THE MAGNETOHYDRODYNAMIC PERISTALTIC MOTION WITH A UNIFORM POROUS MEDIUM IN THE PRESENCE OF SLIP EFFECT. JORDAN JOURNAL OF MECHANICAL AND INDUSTRIAL ENGINEERING (JJMIE) 2015: 9 (4):269 – 278.

- [16] KOTHANDAPANI, M., PRAKASH, J., PUSHPARAJ, V., 2015, "ANALYSIS OF HEAT AND MASS TRANSFER ON MHD PERISTALTIC FLOW THROUGH A TAPERED ASYMMETRIC CHANNEL," *JOURNAL OF FLUIDS*, 2015, 1-9. DOI. [HTTP://DX.DOI.ORG/10.1155/2015/561263](http://dx.doi.org/10.1155/2015/561263)
- [17] GANGAVATHI P, SUBBA REDDY M V, RAMAKRISHNA PRASAD. PERISTALTIC FLOW OF A PRANDTL FLUID IN AN ASYMMETRIC CHANNEL UNDER THE EFFECT OF MAGNETIC FIELD. *INTERNATIONAL JOURNAL OF CONCEPTIONS ON COMPUTING AND INFORMATION TECHNOLOGY* 2014: 2(1):26-31.
- [18] NOREEN SHER AKBAR, NADEEM S, CHANGHOON LEE. PERISTALTIC FLOW OF A PRANDTL FLUID MODEL IN AN ASYMMETRIC CHANNEL. *INTERNATIONAL JOURNAL OF THE PHYSICAL SCIENCES* 2012:7(5): 687 – 695. [HTTPS://DOI.ORG/10.5897/IJPS11.1375](https://doi.org/10.5897/IJPS11.1375)
- [19] KUMAR M A, SREENADH S, SARAVANA R, REDDY R H, KAVITHA A. INFLUENCE OF VELOCITY SLIP CONDITIONS ON MHD PERISTALTIC FLOW OF A PRANDTL FLUID IN A NON-UNIFORM CHANNEL. *MALAYSIAN JOURNAL OF MATHEMATICAL SCIENCES* 2016: 10(1): 35–47.
- [20] NADEEM S, RIAZ A, ELLAHI R. SERIES SOLUTION OF THREE DIMENSIONAL PERISTALTIC FLOW OF PRANDTL FLUID IN A RECTANGULAR CHANNEL. *J APPLMECH ENG.* 2014: 3: 139. DOI. [HTTP://DOI.ORG/10.4172/2168-9873.1000139](http://doi.org/10.4172/2168-9873.1000139)
- [21] RAHMAT ELLAHI, ARSHAD RIAZ N S. PERISTALTIC FLOW OF A PRANDTL FLUID MODEL IN AN ASYMMETRIC. *APPL NANOSCI.* 2014: 4:753–760. DOI. [HTTPS://DOI.ORG/10.1007/S13204-013-0255-4](https://doi.org/10.1007/s13204-013-0255-4)
- [22] ALSAEDI A, NAHEED BATOOL H, YASMIN B, HAYAT T. CONVECTIVE HEAT TRANSFER ANALYSIS ON PRANDTL FLUID MODEL WITH PERISTALSIS. *APPLIED BIONICS AND BIOMECHANICS* 2013: 10: 197–208. DOI. [HTTP://DX.DOI.ORG/10.3233/ABB-140084](http://dx.doi.org/10.3233/ABB-140084)
- [23] SIVAIAH R AND HEMADRI REDDY R. INFLUENCE OF SLIP CONDITIONS ON THE PERISTALTIC TRANSPORT OF A CONDUCTING PRANDTL FLUID IN A POROUS NON-UNIFORM CHANNEL. *INTERNATIONAL JOURNAL OF PURE AND APPLIED MATHEMATICS* 2017: 113 (6):280 – 288.
- [24] NADEEM S, HINA S ADAFA, NOREEN SHER AKBAR B. ANALYSIS OF PERISTALTIC FLOW FOR A PRANDTL FLUID MODEL IN AN ENDOSCOPE. *JOURNAL OF POWER TECHNOLOGIES* 2014: 94 (2): 1–11.
- [25] OGULU T A. EFFECT OF HEAT GENERATION ON LOW REYNOLDS NUMBER FLUID AND MASS TRANSPORT IN A SINGLE LYMPHATIC BLOOD VESSEL WITH UNIFORM MAGNETIC FIELD. *INTERNATIONAL COMMUNICATIONS IN HEAT AND MASS TRANSFER* 2006: 33(6):790–799. V. DOI. [HTTP://DX.DOI.ORG/10.1016/J.ICHEATMASSTRANSFER.2006.02.002](http://dx.doi.org/10.1016/j.icheatmasstransfer.2006.02.002)
- [26] ELDABE N T M, EL-SAYED M F, GHALY A Y, SAYED H M. MIXED CONVECTIVE HEAT AND MASS TRANSFER IN A NON-NEWTONIAN FLUID AT A PERISTALTIC SURFACE WITH TEMPERATURE-DEPENDENT VISCOSITY. *ARCHIVE OF APPLIED MECHANICS* 2008: 78(8): 599–624. VI. DOI. [HTTP://DX.DOI.ORG/10.1007/S00419-007-0181-6](http://dx.doi.org/10.1007/s00419-007-0181-6)
- [27] SRINIVAS S, KOTHANDAPANI M. THE INFLUENCE OF HEAT AND MASS TRANSFER ON MHD PERISTALTIC FLOW THROUGH A POROUS SPACE WITH COMPLIANT WALLS. *APPLIED MATHEMATICS AND COMPUTATION* 2009: 213(1):197–208. DOI. [HTTP://DX.DOI.ORG/10.1016/J.AMC.2009.02.054](http://dx.doi.org/10.1016/j.amc.2009.02.054)
- [28] ABBASI F M, HAYAT T, AHMAD B, CHEN B. PERISTALTIC FLOW WITH CONVECTIVE MASS CONDITION AND THERMAL RADIATION. *J. CENT. SOUTH UNIV.* 2015: 22: 2369–2375. VII. DOI. [HTTPS://DOI.ORG/10.1007/S11771-015-2762-9](https://doi.org/10.1007/s11771-015-2762-9)
- [29] RAVIKUMAR S. ANALYSIS OF HEAT TRANSFER ON MHD PERISTALTIC BLOOD FLOW WITH POROUS MEDIUM THROUGH COAXIAL VERTICAL TAPERED ASYMMETRIC CHANNEL WITH RADIATION – BLOOD FLOW STUDY. *INTERNATIONAL JOURNAL OF BIO-SCIENCE AND BIO-TECHNOLOGY* 2016: 8(2): 395–408. DOI. [HTTPS://DX.DOI.ORG/10.14257/IJBSBT.2016.8.2.28](https://dx.doi.org/10.14257/IJBSBT.2016.8.2.28)
- [30] ABD-ALLA A M, ABO-DAHAB S M, ELSAGHEER M. INFLUENCE OF MAGNETIC FIELD AND HEAT AND MASS TRANSFER ON THE PERISTALTIC FLOW THROUGH A POROUS ROTATING MEDIUM WITH COMPLIANT

- WALLS. *MULTIDISCIPLINE MODELING IN MATERIALS AND STRUCTURES* 2017: 13(4):.648-663. DOI. [HTTPS://DX.DOI.ORG/10.1108/MMMS-05-2017-0031](https://dx.doi.org/10.1108/MMMS-05-2017-0031)
- [31] HAYAT T, SAIMARANI, ALSAEDI A, RAFIQ M. *RADIATIVE PERISTALTIC FLOW OF MAGNETO NANOFLUID IN A POROUS CHANNEL WITH THERMAL RADIATION. RESULTS IN PHYSICS* 2017:7: 3396-3407. DOI. [HTTPS://DOI.ORG/10.1016/J.RINP.2017.07.074](https://doi.org/10.1016/j.rinp.2017.07.074)
- [32] RAMESH K. *INFLUENCE OF HEAT AND MASS TRANSFER ON PERISTALTIC FLOW OF A COUPLE STRESS FLUID THROUGH POROUS MEDIUM IN THE PRESENCE OF INCLINED MAGNETIC FIELD IN AN INCLINED ASYMMETRIC CHANNEL. JOURNAL OF MOLECULAR LIQUIDS* 2016:219: 256-271. VIII. DOI. [HTTPS://DX.DOI.ORG/10.1016/J.MOLLIQ.2016.03.010](https://dx.doi.org/10.1016/j.molliq.2016.03.010)
- [33] SHEIKHOESLAMI M, GANJI D D, JAVED M Y, ELLAHI R. *EFFECT OF THERMAL RADIATION ON MAGNETOHYDRODYNAMIC NANOFLUID FLOW AND HEAT TRANSFER BY MEANS OF TWO PHASE MODEL. J MAGN MAGN MATER.* 2015: 374: 36-43. DOI. [HTTPS://DOI.ORG/10.1016/J.AEJ.2017.02.010](https://doi.org/10.1016/j.aej.2017.02.010)
- [34] RAVI KUMAR S, AMEER AHAMAD N. *JOULE HEATING AND MASS TRANSFER ON MHD PERISTALTIC HEMODYNAMIC JEFFERY FLUID WITH POROUS MEDIUM IN A TAPERED VERTICAL CHANNEL-BLOOD FLOW ANALYSIS MODEL. INTERNATIONAL JOURNAL OF BIO-SCIENCE AND BIO-TECHNOLOGY* 2017: 9(1): 1-22. DOI. [HTTP://DOI.ORG/10.14257/IJBSBT.2016.9.1.01](http://doi.org/10.14257/IJBSBT.2016.9.1.01)
- [35] ABBASI F M, SHEHZAD S A. *CONVECTIVE THERMAL AND CONCENTRATION TRANSFER EFFECTS IN HYDROMAGNETIC PERISTALTIC TRANSPORT WITH OHMIC HEATING. JOURNAL OF ADVANCED RESEARCH* 2017:8 (6):655-661. DOI. [HTTP://DX.DOI.ORG/10.1016/J.JARE.2017.08.003](http://dx.doi.org/10.1016/j.jare.2017.08.003)
- [36] PATEL M, TIMOL M G. *THE STRESS STRAIN RELATIONSHIP FOR VISCOUS-INELASTIC NON-NEWTONIAN FLUIDS, INT. J. APPL. MATH. MECH.* 2010: 6(12): 79- 93. IX.